

Article

Evolution of the Late Mesozoic Magmatism of the Omulevka Terrane of the North Part of the Verkhoyansk–Kolyma Orogenic Region

Vera A. Trunilina

Diamond and Precious Metal Geology Institute, SB RAS, 677980 Yakutsk, Russia;
trunilina40@mail.ru; Tel.: +7-9141016992

Abstract: This article presents the results of a study of Late Mesozoic intrusive formations of the Omulevka terrane of the Verkhoyansk–Kolyma orogenic region. The research area covers the Selennyakh block of the Omulevka terrane and the territory adjacent to the south. The compositions of rock-forming, accessory and restitic minerals and geochemical features of intrusive rocks are considered. The methods of optical microscopy, microprobe, silicate and spectral analyses were used. There are the following several stages in the evolution of magmatism: (1) the Late Jurassic supra-subduction (gabbro, dolerites), (2) the beginning of the Early Cretaceous-transitional from supra-subduction to marginal-continental (gabbro-diorites, diorites, granodiorites), (3) the Early Cretaceous of active continental margin (granodiorites, granites), (4) the Late Cretaceous postorogenic or continental-riftogenic (alkali-feldspar granites of A-type), (5) the Late Cretaceous continental riftogenic (subalkaline gabbroids and basaltoids). In the process of evolution from stage one to stage four, there was an increase in the silicic acid content, total alkalinity and ferruginosity of rocks with the movement of magmogenesis levels to higher and higher horizons of the lithosphere (calculated pressure from 1.6–1.4 GPa to 0.6–0.9 GPa). At the same time, the preservation of high temperatures of magmogenesis (1000–1150 °C) and crystallization implies the supply of additional heat from an external (deep) source during the formation of granitoid melts. The magmatic activity is completed by the intrusion of subalkaline derivatives of a deep hearth, formed by metasomatized lherzolites. All the studied igneous rocks are either direct mantle fusions, or bear signs of the participation of mantle matter in the generation of parent melts in crustal substrates: the presence of tschermakite in gabbroids, nonequilibrium structures, the composition of early generations of biotites corresponding to biotites of mantle and crust–mantle derivatives, the presence of pyroxenes and accessory minerals characteristic of mantle magmas in granitoids. In the diagram Al–Na–K–2Ca–Fe + Ti + Mg, the composition points of the studied intrusive rocks tend to the mixing trend. In general, the research results suggest that the evolution of the Late Mesozoic intrusive magmatism of the studied territory and the specific matter of rock compositions were caused by the crust–mantle interaction as a result of the rise of mantle diapirs in the crust from a long-existing deep hearth of the main melt.



Citation: Trunilina, V.A. Evolution of the Late Mesozoic Magmatism of the Omulevka Terrane of the North Part of the Verkhoyansk–Kolyma Orogenic Region. *Minerals* **2021**, *11*, 1208. <https://doi.org/10.3390/min11111208>

Academic Editor: Huan Li

Received: 1 September 2021

Accepted: 27 October 2021

Published: 29 October 2021

Publisher's Note: MDPI stays neutral with regard to jurisdictional claims in published maps and institutional affiliations.

Keywords: gabbroids; granitoids; mineralogy; geochemistry; melts; magmogenesis parameters; mantle–crustal interaction; Verkhoyansk–Kolyma orogenic area



Copyright: © 2021 by the author. Licensee MDPI, Basel, Switzerland. This article is an open access article distributed under the terms and conditions of the Creative Commons Attribution (CC BY) license (<https://creativecommons.org/licenses/by/4.0/>).

1. Introduction

The Verkhoyansk–Kolyma orogenic region is characterized by the intensive development of Late Mesozoic magmatism. There are small bodies and dike series of variegated composition and numerous bodies of granitoids forming longitudinal belts elongated parallel to the boundaries of the main tectonic structures (main and northern), and transverse ones, oriented across or at an angle to them. The main batholith belt stretches in a north-western direction for a distance of about 1000 km along the border of the Polousno-Debin terrane and the marginal terranes of the composite Kolyma–Omolon microcontinent (superterrane). It also includes the Cretaceous granitoids of the Selennyakh block of the Omulevka

marginal terrane considered in the work (Figure 1) [1]. The Cretaceous granitoids of the Selennyakh river basin considered in this work also belong to it.

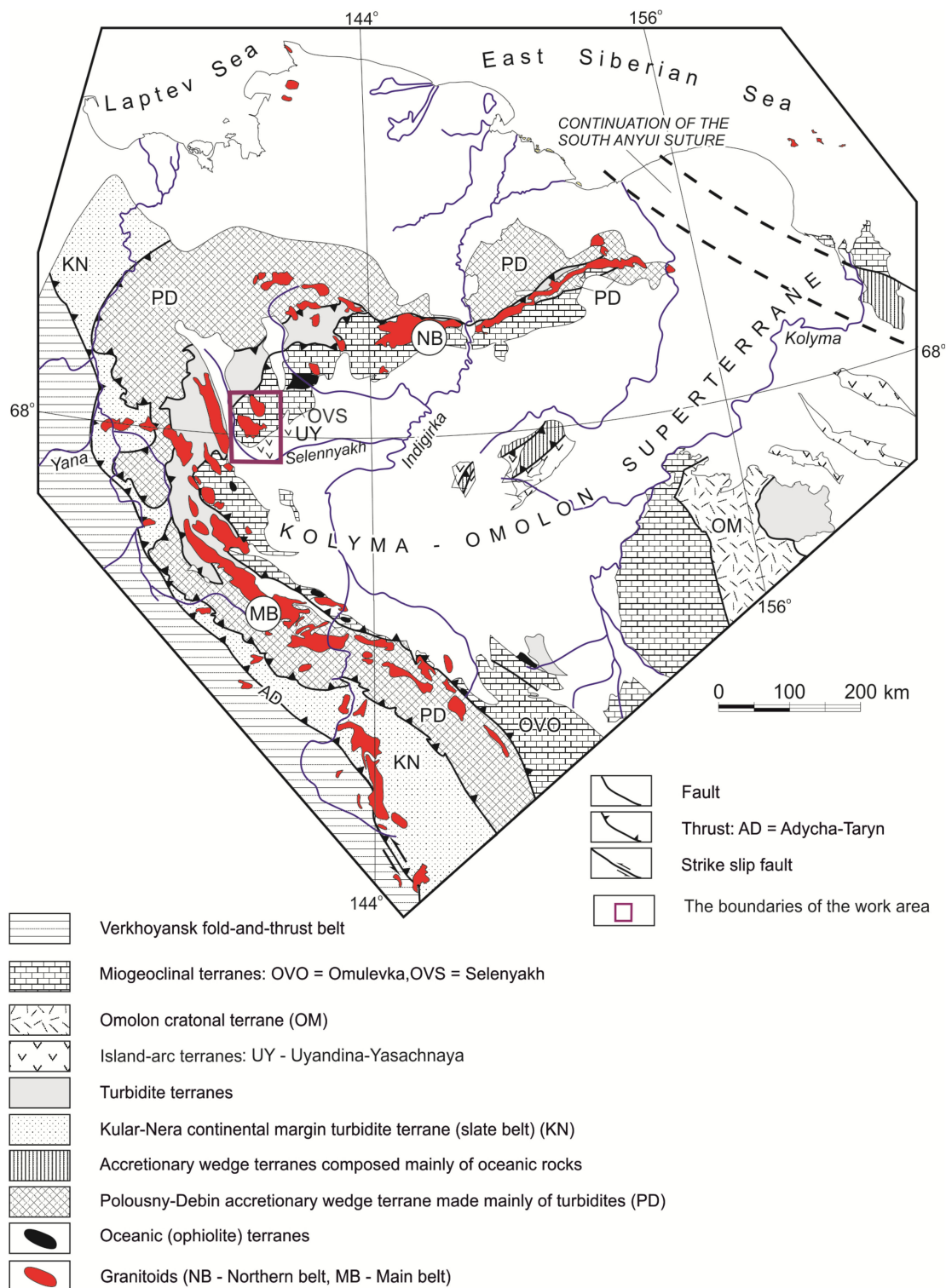


Figure 1. Tectonic map of the northeastern Verkhoyansk–Kolyma orogenic belt [1].

Despite the long-term study of the granitoid magmatism of the orogenic region, many questions of the genesis of granitoids remain controversial. This primarily concerns the role of deep sources in magmogenesis processes and the causes of the petrographic

diversity of granitoids. For a long time, all the granitoids of the region were considered as crustal, while their diversity was explained by various reasons, and their formation was related to orogenic processes. In this article, the author has tried to approach the solution of these issues.

At the early stages of studying the territory, the granitoids of the Main belt were assigned to the Kolyma Late Jurassic–Early Cretaceous complex [2,3], or the formation of calcium-poor granites of crustal origin [4]. The similarity of the parent melts for them was assumed, and the petrographic diversity was explained by the processes of contamination of the host rocks of a different composition. Later, the following three associations of granitoids were identified as part of the Main belt: (1) Late Jurassic–Early Cretaceous granodiorite-granite association, (2) Late Jurassic–Early Cretaceous granite-leucogranite association, (3) Late Cretaceous association of high-aluminous granites. The specific nature of granitoids was associated with the values of geothermal gradients and the composition of the basement during magma formation [5]. The question of the presence of not only crustal but also mantle-crustal formations in the granitoids of the Main belt, was not even raised. The author of the proposed article, based on many years of research, identifies the Late Jurassic suprasubduction granitoids of the M-type of gabbro-tonalite-granodiorite association within the Main belt; formed at the turn of the Jurassic and Cretaceous mantle-crustal granitoids of the I-type of diorite-granodiorite-granite association; the Early Cretaceous crustal granites of IS- and S-types of granodiorite-granite and granite-leucogranite associations; the Late Cretaceous alkaline-feldspar granites of A-type, successively replacing each other in the process of the evolution of the orogenic region [6].

The territory of the Selennyakh tectonic block and its nearby area attracts by the fact that numerous outcrops of intrusive rocks of various composition and age are concentrated here on a relatively small territory in the Selennyakh River basin. The study of not only granitoids, but also the basic rocks preceding and following them, allows us to identify the evolution of geodynamic settings and general genetic aspects of the formation of magmatism.

The proposed work presents the results of studying the geological position, petrography, mineralogy and chemical composition of derivatives of pre-granitoid basic magmatism, granitoid magmatism and post-granitoid sub-alkaline magmatism of the Selennyakh block and the following genetic conclusions from them.

2. Methods

A study of granitoid massifs was carried out by the method of vertical and horizontal sections to obtain data on changes in rock compositions from the center of the bodies to their contacts and from the most eroded horizons to the apical ones (Figure S1). Dikes were traced by the dip and strike. More than 250 samples were taken for petrographic studies and the determination of the chemical composition of all types of rocks. In addition, 30 bulk samples (4–5 kg each) were selected, and monofractions of dark-colored minerals were extracted from them. Tables S1–S4 show analyses of unchanged or relatively unchanged rocks and minerals. Petrography of granitoid massifs and dikes was studied using an Olympus optical microscope (BX50, Leica, Wetzlar, Germany), allowing conclusions to be drawn regarding the crystallization and evolution paths of the melts. The composition of rock-forming and accessory minerals was studied using an X-ray microanalyzer Camebax-micro (Cameca, Saint-Denis, France) and a scanning microscope Jeol JSM-6480LV (JEOL, Tokyo, Japan).

Complete whole-rock geochemical analyses and quantitative spectral and inductively coupled plasma-mass spectrometry (ICP-MS) analyses of element contents of ores were performed, followed by mathematical processing of the data using CGDkit, Igpct and PetroExplorer software (version 2) [7–9]. On this basis, we determined the conditions of the generation and crystallization of the melts.

Feldspars were studied using optical methods with an E.S. Fedorov stage (Fedorov method) [10], enabling the determination of zoning patterns and the structural ordering

of minerals (the Fedorov method consists of determining the shape and orientation of the optical indicatrix in a crystal; the degree of structural (or crystal) ordering is the amount of deviation of the real (observed) spatial lattice of a crystal from the ideal (theoretical) spatial lattice. It decreases with an increasing temperature [10,11].

All analyses except ICP-MS were conducted at the Diamond and Precious Metal Geology Institute (DPMGI) (SBRAS), Yakutsk, Russia. Chemical compositions of the rocks were determined using conventional wet-chemistry analytical techniques. The chemical composition and characteristics of minerals and rocks of the studied samples are given in Tables S1–S4. The ICP-MS analysis to determine the contents of La, Ce, Sm, Yb was conducted at the Geochemistry Institute of the Siberian Branch of the Russian Academy of Sciences (SB RAS) Irkutsk, with the use of a high-resolution ELEMENT 2 mass spectrometer (version Finangan Element2, Thermo Quest Finnigan MAT, Bremen, Germany). Isotope studies of Rb-Sr were performed on an MI-1201-T mass spectrometer (electron optics, Sumy, Ukraine) in single-beam mode using tantalum ribbons. Rb concentrations were calculated by isotope dilution, and those of Sr by double isotope dilution. Sr isotope composition was estimated without adding an indicator. Chemical treatment of samples included decomposition in a mixture of HF + HClO₄ (3:1) in Teflon bombs in autoclave mode at a temperature of 200 °C for 8 h. Elements were separated using the ion-exchange chromatography method with the use of Dowex resin, 50 × 8200 mesh. The error in measuring the isotope ratios did not exceed 0.05%.

3. Geological Setting

The studied area is located within the Verkhoyansk–Kolyma orogenic region. According to the concept of plate tectonics, the region records the Verkhoyansk fold-thrust belt, adjacent to the Siberian craton from the west, the Kolyma-Omolon microcontinent (or composite superterrane) in the east and the Okhotsk terrane in the southeast [1,12,13]. The Kolyma-Omolon microcontinent is a collage of terranes of various nature. It was attached to the North Asian craton at the end of the Late Jurassic—the beginning of the Early Cretaceous with the formation of extended granitoid belts—the main one with an isotopic model Sm-Nd age of 152–145 Ma and the northern one with an age of 135–127 Ma [1,14,15]. Along the southwestern and northwestern margins of the Kolyma-Omolon microcontinent, the Omulevka continental regional terrain is extended (Figure 1). The Omulevka terrane is divided into several tectonic blocks, one of the largest of which is the Selennyakhsky block, within which the studied Mesozoic magmatic formations are localized. The Selennyakh block is composed of Early–Middle Paleozoic carbonate and terrigenous-carbonate sediments, pre-Ordovician marbles, amphibolites, amphibole-biotite and two-mica schists, plagiogneisses and green schists. The Upper Paleozoic, Triassic and Lower–Middle Jurassic deposits are insignificant and represented by siltstones and mudstones with rare interlayers of sandstones, limestones, marls, andesite and basalt flows.

In the center of the Selennyakh block, the following three granitoid massifs are exposed: Syachan, Sakhanya and Kuturuk, with areas of 700 km², 400 km² and 40 km², respectively (Figure 2). Granodiorites predominate in the Sakhanya and Kuturuk massifs, and granites prevail in the Syachan massif. At contact with terrigenous rocks, fine-grained leucocratic granites are observed; at contact with carbonate rocks, there is a zone of endo- and exoskarns of monzonite, granosyenite and K-feldspar-pyroxene composition [6]. The massifs are accompanied by aplite and leucogranite dikes. Dikes and small stocks of granodiorite-porphyry and granite-porphyry are confined to numerous fault zones. Table 1 shows the results of determining the age of rocks performed by A.I. Zaitsev based on the samples of the author. The ⁴⁰Ar-³⁹Ar isotopic age of granodiorites of the Sakhanya massif is 142–132 Ma, and that of granites—136–134 Ma [14]. Granites along fault zones and granite-porphyry dikes are intensely greisenized and impregnated with cassiterite and wolframite. Calcareous boron-bearing skarns with Sn-W mineralization are developed after terrigenous-carbonate rocks. Quartz-chlorite-carbonate metasomatites have associated gold-base metal mineralization with accompanying tin.

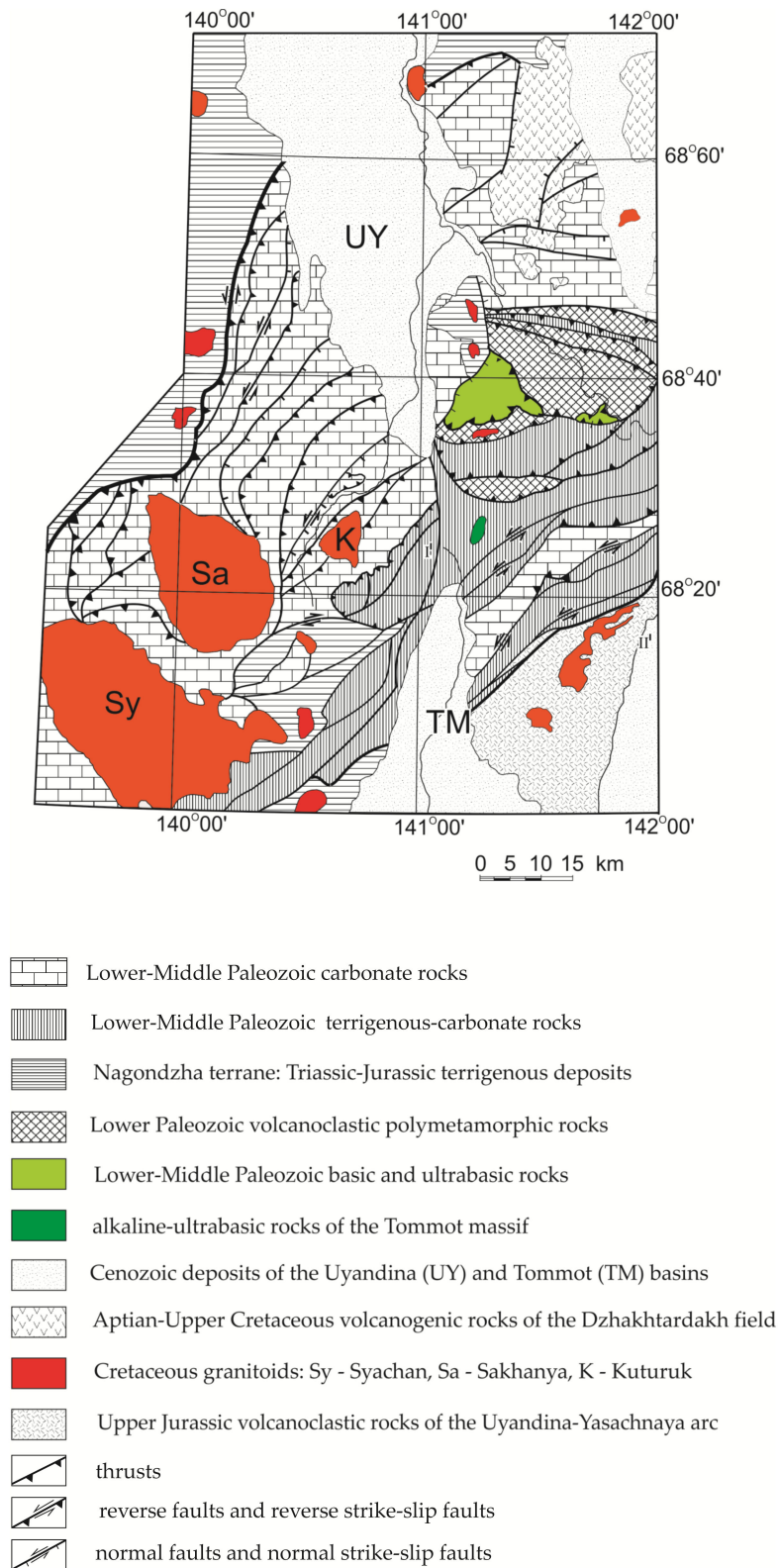


Figure 2. Structure of the Selennyakh block of the Omulevka terrane [1].

Table 1. The isochronous age of magmatic rocks.

The Rocks	The Isochronous Rb-Sr Age	I ₀	K-Ar Age
Dolerite (dike)	158 ± 11	0.7067 ± 0.0005	169 ± 9
Gabbro-diorite (stock)	155 ± 5	0.7069 ± 0.0005	
Granodiorite of Agdai massif	148 ± 6	0.7092 ± 0.0004	146 ± 2
Leucogranite of Agdai massif	92 ± 3	0.7184 ± 0.0029	100 ± 2
Granodiorite of Kuturuk massif	142 ± 6	0.71408 ± 0.00025	146 ± 4
Granodiorite of Sakhanya massif	136 ± 1	0.71349 ± 0.00038	132 ± 2
Granite of Syachan massif	126 ± 4	0.7107 ± 0.0004	125 ± 1
Granite-porphyrity of Syachan massif	122 ± 3	0.7149 ± 0.0005	122 ± 1
Granite-porphyrity of Ust-Burgokhchan massif	91 ± 3	0.71053 ± 0.00023	
Rhyolite-porphyrity of Burgokhchan massif	102 ± 12	0.7254 ± 0.0014	

In the southern part of the studied territory, mainly volcanogenic-sedimentary formations of the Uyandina-Yasachnaya ensialic paleo-island arc are exposed [16,17] (Figure 3).

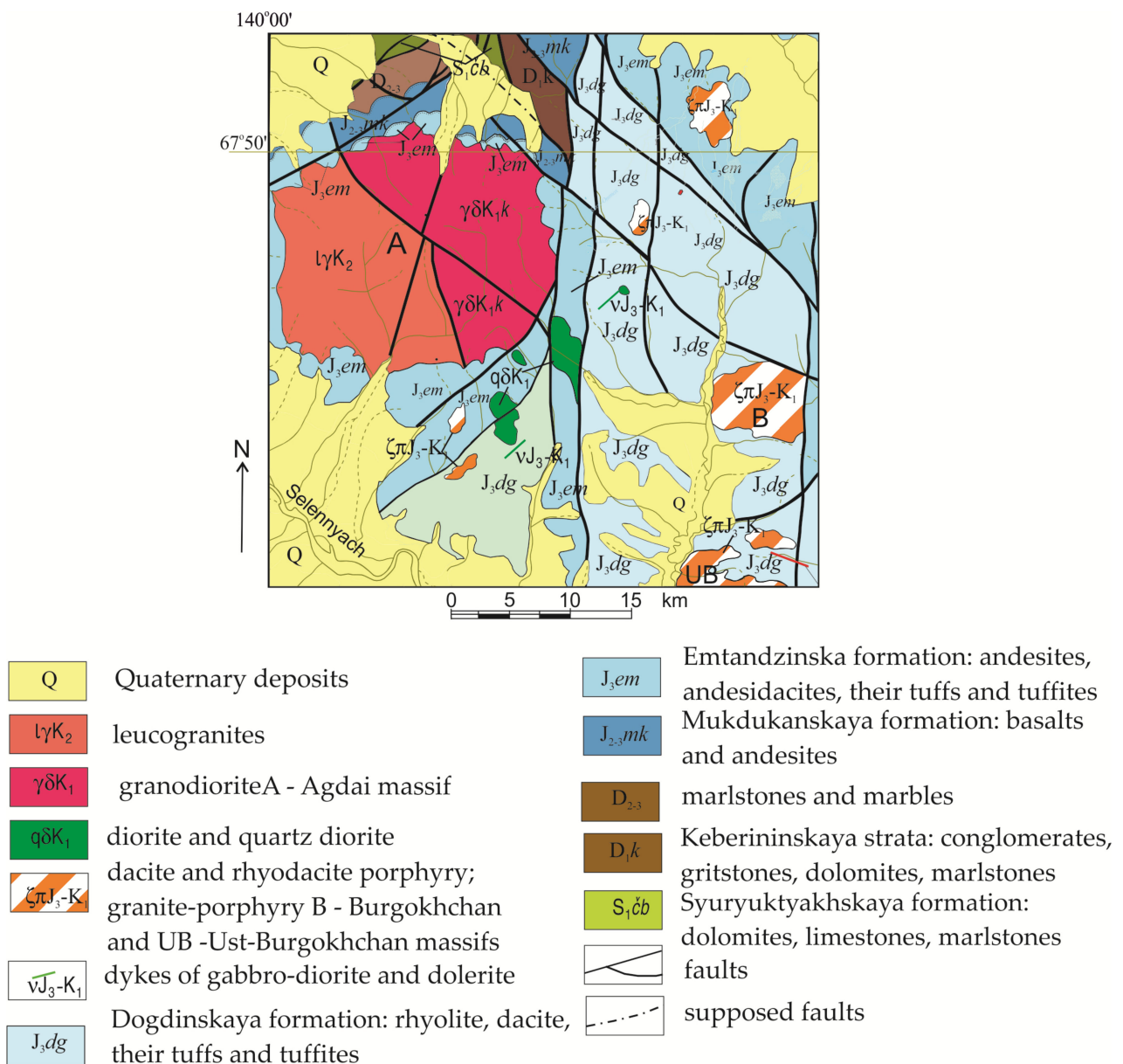


Figure 3. Geological map of the Agdaisky region.

At the base of the volcanogenic-sedimentary strata lies a substantially andesite formation with a subordinate number of basalts, tuffs and tuff lavas of medium and basic composition. The total thickness of the section is 700–900 m. Higher up lies the shale-rhyolite strata with a thickness of up to 500 m. Volcanites are represented by alternating rhyolites, dacites, tuffs and clastolaves of acidic composition. At the top of the section, there are ash tuffs, pyroclastics in the cement of terrigenous rocks, interbeds of carbonaceous claystones, marking the transition to subaerial conditions. The pre-Late Mesozoic base of the belt is a system of blocks and thrust sheets composed of igneous and sedimentary rocks. The volcanogenic-sedimentary strata are intruded by the Agdai massif.

The eastern part of the massif is composed of a complex of rocks from gabbro-diorites to granodiorites, and the western part is composed of leucocratic alkaline-feldspar granites. The isotopic Rb-Sr age of the massif diorites is 148 Ma, alkaline feldspar granites— 92 ± 3 Ma. Earlier, the massif was considered as a multiphase structure with a composition of rocks from gabbro to leucogranites. The formation of the massif is preceded by small gabbro stocks and dolerite dikes with an isotopic K-Ar age of $154\text{--}158 \pm 3$ Ma [18].

Simultaneously, with the western part of the Agdai massif, the formation of the subvolcanic Ust-Burgokhchan and Burgakhchan massifs of leucogranite composition took place. The vein facies are represented by single thin (several cm) veinlets of fine-grained alaskites and aplites. A zone of intensive crushing is traced through the western and central part of the granite outcrop in the north-eastern direction, where both the granites and the host rocks are intensely ferruginated and bear nests of a pitch-black fine-crystalline mineral surrounded by red ochres. The western contact of the massif is tectonic. The Rb-Sr isochronous age of granites is 91 ± 3 Ma—the beginning of the Late Cretaceous [17]. The magmatism of the territory is completed by the intrusion of dikes and small rods of trachydolerites and trachyandesites with an isotopic K-Ar age of 79–69 Ma [18].

4. Petrography and Mineralogy of Magmatic Rocks

The earliest intrusive formations of the Mesozoic in the Selennyakh River basin are small stocks, chonoliths, dikes, sills of gabbro, gabbro-dolerites, dolerites and gabbro-diorites, lying within volcanogenic sedimentary rocks of the Late Jurassic [18]. Xenoliths of metamorphosed Jurassic andesites are frequently found in them. The rocks are massive and trachytoid, with diabase, poikilophytic structures, porphyric and glomeroporphyric structures in dikes and a microdiabasic, dolerite, occasionally intersertal basis. Usually, the rocks are intensively modified (chlorite-carbonate-epidote facies of propylitization). Near the contacts of granite plutons, they are schistosed and broken down, with the development of contact biotite or quartz-biotite aggregates. The main minerals of the rocks are plagioclase and pyroxene. In porphyric rocks, they form phenocrysts with mutual inclusions in each other, and in medium-grained rocks, they have either a close degree of idiomorphism, or pyroxene fills angular gaps between idiomorphic plagioclase grains. Plagioclase is non-zonal or with indistinct direct zoning (from 66% to 40% an). Labrador predominates (50–58% an) a medium and high degree of structural ordering (0.5–0.8), with the cores of the most ordered being bitownite (78–85% an). Pyroxene is a magnesian augite with a calculated crystallization temperature from 1196 °C to 980 °C [19], which is lower than the liquidus temperature of the dry melt (Table S1). Sporadically, forsterite relics are found (Fo 84.3, Fa 15.7; Fo 82.2, Fa 17.8). Inclusions of a chromium spinel are noted in olivine from the dolerites dike (Al_2O_3 , 17.99%; Cr_2O_3 , 47.68%).

Pyroxenes are replaced by hornblende ($f = 45\text{--}66\%$), which crystallizes in the temperature range of 850–810 °C and at a pressure from 4.4 kbar to 2.2 kbar from a water-saturated melt with a water content of 5.2–5.8% (Table S2) [20,21]. In porphyric rocks, it is present only in the groundmass. The substitution of pyroxene for high-alumina amphibole, chermakite, probably restite, was noted. Biotite is found in the form of single grains developed by pyroxene or amphibole. It is represented by eastonite-annite varying from moderate to high ferruginosity (Table S3) [22–27]. The calculated crystallization temperatures were from 725 °C to 685 °C [22]. The composition parameters are similar to those of

biotites of the Early Cretaceous granitoids. This allows us to assume a post-magmatic, contact-metamorphic origin of biotites. The accessory fraction is dominated by high-temperature titanomagnetite (TiO_2 to 15%, SiO_2 to 7.3%) and Cl-apatite (to 1.76% Cl). In the post-magmatic stage, plagioclase deaorthitization occurs (up to albite), as well as the replacement of dark colors with a serpentine-like mineral, a fibrous actinolite and a chlorite of the delessite group.

At the beginning of the Early Cretaceous, the formation of the Agdai massif of complex composition began. The eastern part of the Agdai massif is composed of diorites, quartz diorites and granodiorites with gradual transitions between them. The xenoliths contain gabbro-diorites. The massif cover is inclined to the south-east, where a number of small satellites of mainly diorite composition can be traced. The vein facies is represented by fine-grained granites and aplites. The western part of the massif is composed of leucocratic alkaline-feldspar granites. Earlier, the massif was considered as a multiphase structure with a composition of rocks from gabbro to leucogranites. The formation of the massif is preceded by small gabbro stocks and dolerite dikes.

Rocks of the eastern part of the Agdai massif are shlirovo-taxite, with a combination of sites of different composition, structure and different grain sizes. In rocks of diorite composition, idiomorphic labradorite grains are the first to crystallize (50–58% an) and magnesioaugite (ferruginosity $f = 22\text{--}24\%$, Table S1) forms panidiomorphic-granular autoliths. The gaps between them are filled with subidiomorphic grains of amphibole, zonal andesine oligoclase (44–22% an) and quartz, or a fine-grained pegmatite aggregate. The amphibole, magnesio-hornblende ($f = 45.4\text{--}47.8\%$), as a rule, is replaced by cannitoite. It crystallizes in an oxidizing environment when the water content in the melt is 4.7% [20,21]. Grains of restitic tschermakite are also found. Biotite is a moderately ferruginous, low-alumina eastonite-annite. It begins to crystallize together with amphibole and oligoclase when there is high water and chlorine activity and the water content in the melt is 3.5–4%, and it ends after quartz, to which interstitial grains are sometimes confined (Table S3). The most high-temperature generation in terms of composition parameters correspond to biotites of mantle and crustal–mantle derivatives (Figure 4) [28–30]. A potassium-sodium feldspar is observed as part of a xenomorphic-granular or micropegmatite aggregate. It is represented by a crypto- and micropertite intermediate-to-low microcline with a content of ab up to 22%.

The main accessory minerals are titanomagnetite (7.4% TiO_2 , 4.4% SiO_2), magnetite, allanite, magnesium ilmenite (2–5% MgO at 0.05–0.2% MnO), apatite, rich in chlorine and fluorine (0.6–0.8% Cl and 3.6–5.4% F), zircon ($\text{ZrO}_2/\text{HfO}_2 = 56\text{--}66$), single grains of pyrope-almandine (29% py).

Granites of dikes are porphyric, with autoliths of an amphibole-plagioclase composition, plunged in a micropegmatite matrix. Plagioclase of autoliths—zonal andesine-oligoclase and oligoclase (30–15% an), amphibole—magnesian-ferruginous hornblende ($f = 47.8\%$).

The massifs of the Early Cretaceous granitoids exposed in the center of the Selenyakh block are composed of amphibole-biotite granodiorites and granites with gradual transitions between them. Granodiorites of endocontacts contain xenoliths of diorites and gabbro-diorites. Pyroxene is found only in endoscarns and has the composition of ferrodiopside, ferroaugite and ferropigeonite with ferruginosity $f = 44\text{--}64\%$ and the calculated crystallization temperature $T = 966\text{--}877\text{ }^\circ\text{C}$ [19].

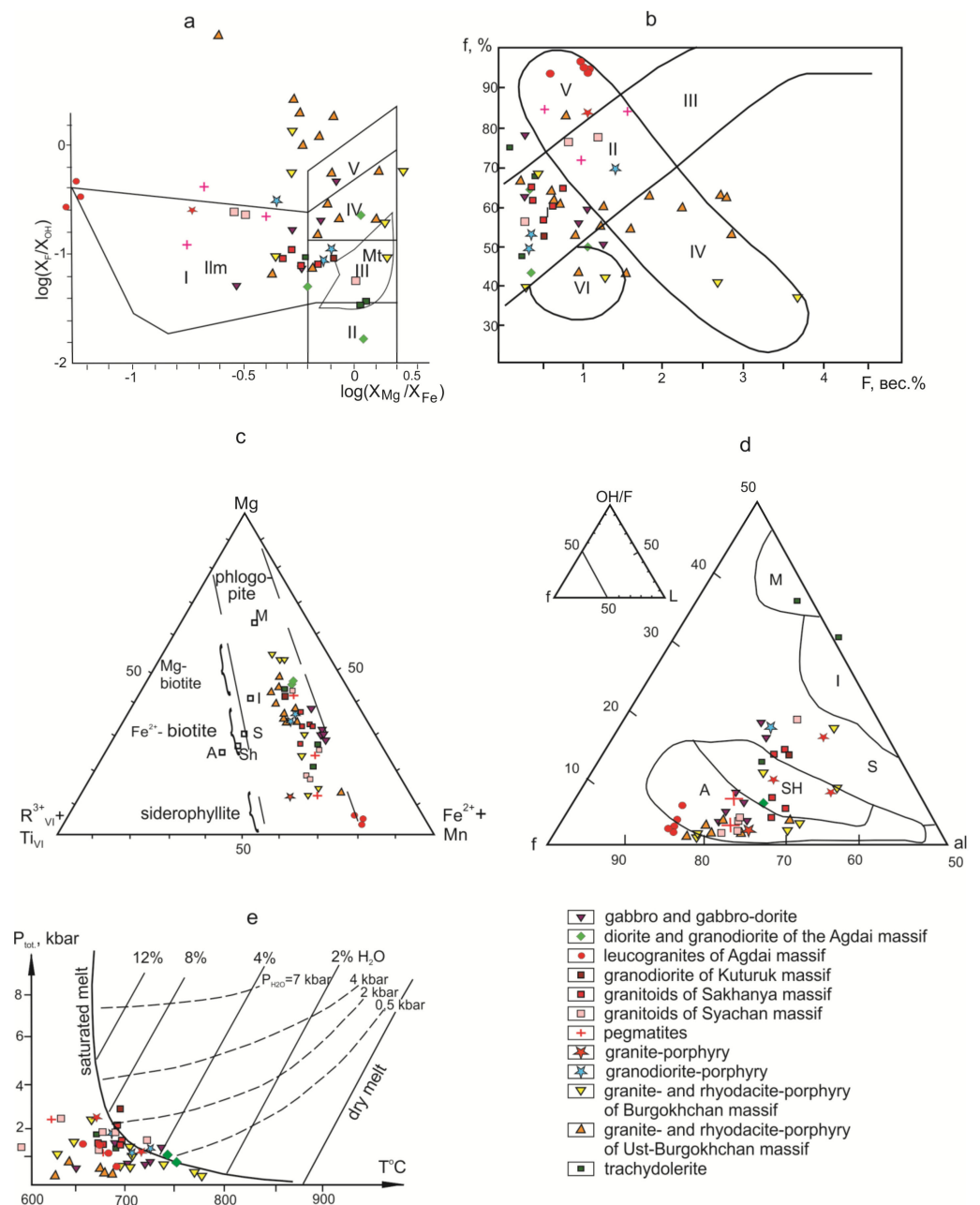


Figure 4. Composition of biotites from magmatic rocks of the Selennyakh River basin: (a) F/OH–Mg/Fe diagram for biotites of magmatic rocks. Fields of biotite derived from melts [28]: I—contaminated and assimilated marine metasediments; II—mantle; III—crustal-mantle; IV—mantle-crustal; V—crustal anatectic; Ilm—ilmenite series of granitoids, Mt—magnetite series of granitoids; (b) F vs. f diagram for biotites. Fields of the diagram [29]: I–II–III—biotites from rocks of granite-leucogranite and granodiorite-granite associations; IV–II–V—gabbro-granite associations; VI—derivatives of mantle magmas; (c) $R^{3+} + Ti$ –Mg– $Fe^{2+} + Mn$ ratio in biotites. $R^{3+} = Fe^{3+} + Al^{3+}$. The field of compositions and points of average compositions of biotite different petrotypes [30]; (d) the fluoride ratio of (OH/F), the aluminum mole fraction (al) and ferruginosity (f) of biotite. Fields of the diagram [30]: biotites of standard types of granitoids: I—mantle-crustal island arcs, M—mantle, S—crustal and mantle-crustal collision environments, SH—post-collisional shoshonite, A—anorogenic environments. (e) P–T diagram of the granite-water system at independent P_{tot} and P_{H_2O} [31].

In granodiorites, the earliest mineral is andesine-labrador composition of 52% an, 39% ab, 9% or, with the crystallization temperature 950 °C [31]. Plagioclase of the periphery (40% an, 53% ab, 7% ort, was formed at 800–780 °C. Together with the middle zones of plagioclase, the hornblende begins to crystallize. It is formed in the temperature range of 846–712 °C, with a pressure from 4.6 kbar to 1 kbar and a water content of 4.1–5.3% in the melt. Its ferruginosity decreases with a decrease in pressure from 55.2% to 43.7%. Then, acid plagioclase (32–20% an, 7–2% ort) and an allotriomorphic-grained biotite-quartz-feldspar aggregate are formed. K-feldspar is represented by an intermediate to low orthoclase and microcline. Magnesian-ferruginous biotite ($f = 51$ –67%), with a decrease in temperature is replaced by ferruginous biotite ($f = 77\%$) (Table S3). In terms of composition, biotite corresponds to that of the crustal granodiorite-granites of the ilmenite series, and only the most highly magnesian varieties correspond to biotites of the mantle-crustal rocks of the ilmenite-magnetite series (Figure 4). Granites differ from granodiorites in the almost complete absence of minerals of the early amphibole-plagioclase paragenesis and the predominance of microcline among K-feldspars.

The accessory minerals of granitoids include ilmenite, F-apatite, zircon, titanite, allanite, garnet and rare magnetite grains. Zircon is mainly represented by low-temperature crustal morphotypes P, with $ZrO_2/HfO_2 = 30$ –60 typical for granodiorites and granites. There are also single crystals of crustal–mantle morphotype D with $ZrO_2/HfO_2 = 68$ –88 [32]. In an intergrowth with the amphibole, the lower crustal pyrope-almandine (up to 29% py) is observed. Later, post-magmatic garnet has the composition of grossular-almandine, which is characteristic of derivatives of water-saturated acid melts and aqueous fluids [33]. Microinclusions of gold are found in amphiboles, and single grains of cassiterite occur in leucogranites at endocontacts.

Aplites and leucogranites are composed of oligoclase (15–22% an, 4–5% ort), cryptoperthitic potassium–sodium feldspar (70–75% ort, 25–30% ab, 0–0.5% an), and siderophyllite. The latter is enriched in fluorine (1.6%) and crystallized from the water-saturated melt (Table S3, Figure 4). These rocks often contain pockets of quartz-feldspar pegmatites of up to 15 cm in diameter. They contain large scales of ferruginously eastonite-annite or siderophyllite, nests of schorl and fluorite in association with muscovite and cassiterite.

Granite- and granodiorite-porphyrries have a porphyritic and glomeroporphyritic texture. The phenocrysts in the porphyry granite are composed of quartz, biotite and, occasionally, hornblende. Biotite is completely replaced by fine siderophyllite flakes ($f = 85\%$). The accessories include ilmenite, fluorapatite, zircon, fluorite and thorite. Porphyritic phenocrysts of granodiorite-porphyry are composed of andesine-labradorite (56–45% an), hornblende and biotite, similar to those of granodiorites. The accessories include ilmenite, magnetite, chlor-apatite and fluor-apatite, zircon of morphotypes D and P, titanite, allanite and pyrite, arsenopyrite. Quartz-chlorite-carbonate metasomatites also contain galena and sphalerite. The greisenized rocks are characterized by tourmaline, fluorite, cassiterite and wolframite.

At the turn of the Early and Late Cretaceous, the western part of the Agdai massif and the subvolcanic Burgokhchan and Ust-Burgokhchan massifs of alkaline-feldspar granites and leucogranites and a series of dikes of rhyolite and rhyodacite porphyry were formed [17]. The vein facies of the massifs are represented by rare thin veinlets of fine-grained porphyry-like leucogranites and aplites. The western part of the Agdai massif is in contact with the eastern part through a system of faults. It is composed mainly of medium-grained granites of a hypidiomorphic granular texture. The marginal parts of the Burgokhchansky and Ust-Burgokhchansky massifs are porphyry and glomeroporphyry with microgranite, micropegmatite or felsite groundmass.

The rocks of all the massifs are characterized by a high-temperature early magmatic association of minerals: sanidine or anorthoclase with composition of 45–50 ab, 48–54 ort and 0.7–1.8 an, and ferrodiorite or ferroaugite located in the form of idiomorphic inclusions in it ($f = 83$ –86%) with a stable presence of the aegirine molecule (0.7–2.7%). The calculated [19] crystallization temperature was 1063–1017 °C at a pressure of 5.8–8.6

kbar. More often, relics of clinopyroxene are identified among the schlieren of amphibole, replacing it in interstices of large anorthoclase grains. Sporadically, rounded fayalite inclusions in sanidine ($f = 80\text{--}90\%$) are also observed. In the second stage, mesoperthite potassium-sodium feldspar with close ratios of albite perthites and high or intermediate orthoclase and oligoclase-albite and isometric and irregular quartz grains in sharply minor amounts are crystallized. Calculations [34] indicate the temperature of the melt at this stage—850–856 °C. In the third stage, xenomorphic quartz grains or fine-grained pegmatite are formed. Amphibole and biotite are late and post-magmatic. They fill interstices between grains of salic minerals or form thin veinlets. They contain numerous inclusions of ore minerals, monazite, allanite, xenotime and undiagnosed small inclusions of radioactive minerals. In porphyry rocks of subvolcanic facies, subeuhedral quartz grains in intergrowth and with inclusions of uniaxial sanidine are the first to crystallize. Groundmass is micropegmatite or microgranite.

Amphibole has a composition of hastingsite or ferriedenite ($f = 74\text{--}100\%$) with a high total alkali content. A high concentration of halogens is its most typomorphic feature (Table S2). The calculated parameters of crystallization are as follows [20,21]: $P = 3.9\text{--}2.1$ kbar, $T = 835\text{--}761$ °C. Biotite begins to crystallize somewhat later than amphibole, replacing it on the periphery of the grains. In the granites of the Agdai massif and the most eroded horizons of the Burgokhchan and Ust-Burgokhchan massifs, biotite has mainly the composition of siderophyllite with a ferruginosity of 86–97%. It crystallizes at 692–641 °C and the water content in the melt is 6–8%. In subvolcanic rocks, its first generation is represented by magnesian and magnesian-ferruginous eastonite-siderophyllite with a ferruginosity of 39–66%. The calculated crystallization temperatures are 777–677 °C with a water content of 2.5–6% in the melt. All biotites are enriched with fluorine and were formed at high activity of water and fluorine (Table S3). The ratio of ferruginosity and fluorine content is comparable to the biotites of late gabbro-granitic differentiates, and low values of OH/F are comparable with biotites of A-type (Figure 4).

Granites of all the studied massifs contain single grains of magnesioaugite ($f = 21\text{--}29\%$) and andesine-labradorite. In terms of low ferruginosity and abnormally high crystallization temperature, magnesioaugite is comparable to clinopyroxenes of picrite–basalt associations of the continents [35]. Corroded grains of ferrygedrite are found here, characteristic of highly metamorphosed rocks.

The accessory fraction is strongly dominated by allanite, which forms small grains and their clusters. Titanomagnetite is also a characteristic accessory mineral of rocks (3–12% TiO_2). In all the samples, small grains of zircon with widely varying $\text{ZrO}_2/\text{HfO}_2$ ratios were also found—from typical for granites to typical for basic rocks (29–128). Rare grains of apatite contain 3.3–6.2% F and 0.07–0.12% Cl. Sulfides—pyrite, arsenopyrite, millerite—are practically devoid of impurities. Single grains of grossular-almandine (54–64% gross) and pyrope-almandine (20.7–20.8% py) are probably restyctic or xenogenic. Single grains of chromite were also found in the crushed sample (30% Cr_2O_3 , 50% Fe_2O_3).

The latest magmatic formations of the territory are represented by single dikes of trachydolerites and trachyandesites. They cut granitoids of the Syachan massif and granite-porphyry of the Ust-Burgokhchan massif. Their thickness ranges from 10–15 cm to 3–4 m. The predominant trachydolerites are massive, porphyry, with diabase and dolerite microgranular groundmass. The rocks are composed of andesine-labrador lathes (50–52% an) and subprismatic grains of pyroxene and hornblende. In the center of the plagioclase grains, corroded bitownite cores with inclusions of idiomorphic pigeonite are sporadically observed. The crystallization temperature of labrador-bitownite ($an\ 71.4\ ab\ 18.6\ ort\ 10$) is determined at 1200 °C [31]. Dark-colored minerals are represented by pyroxene and amphibole, rarely by replaced ferruginous olivine with iddingsite ($f = 56\text{--}59\%$) containing lamellar separations of chromium-containing magnetite (1.1% Cr_2O_3). Pyroxene is represented by ferrodioptase ($f = 37\%$) and more ferruginous clinoenstatite ($f = 68\%$), crystallized at 997–1000 °C (Table S1). Amphibole forms pseudomorphoses on pyroxene with the preservation of close ferruginosity. It has the composition of hornblende and fer-

roedenite with crystallization parameters: $T = 985\text{--}840\text{ }^{\circ}\text{C}$, $P = 2.2\text{--}0.86\text{ kbar}$. It crystallized under oxidizing conditions ($-\log f\text{O}_2 = 10.5$) when the water content in the melt is 3.5% (Table S2). In turn, it is replaced by ferruginous eastonite-annite with $f = 64.2\text{--}78.8\%$. Up to 5–7% of the rock volume is composed of titanomagnetite (6–19.8% TiO_2), forming large idiomorphic grains. Clusters of needle-like chlor-apatite with a chlorine content of up to 1.66% are characteristic.

5. Petrochemistry of Magmatic Rocks

The chemical composition of the earliest igneous rocks of the Late Mesozoic within the Selennyakh block varies from gabbro to diorites (Figure 5, Table S4) [36–39]. They are characterized by a potassium-sodium type of alkalinity (Figures 6 and 7), moderate aluminosity (Figure 8) [40–42] and low ferruginosity ($f = 48\text{--}58\%$). The main parameters of the composition correspond to those of the tholeiitic, less calcareous-alkaline series of island arcs (Figure 9) [43]. Gabbro and dolerites are olivine-diopside normative, with a sharp predominance of normative albite over orthoclase. Diorite porphyrites are hypersthene-diopside normative, with a small amount of normative quartz. The differentiation index DI of rocks is low—24–27% for gabbro, and only in one case—55% (for diorite). According to the classification [44], they belong to the family of tholeites and olivine tholeites. The calculated parameters of magmogenesis determined by different programs [36,37,45–48] are close: $P = 12\text{--}14\text{ kbar}$, $T = 1180\text{--}1220\text{ }^{\circ}\text{C}$.

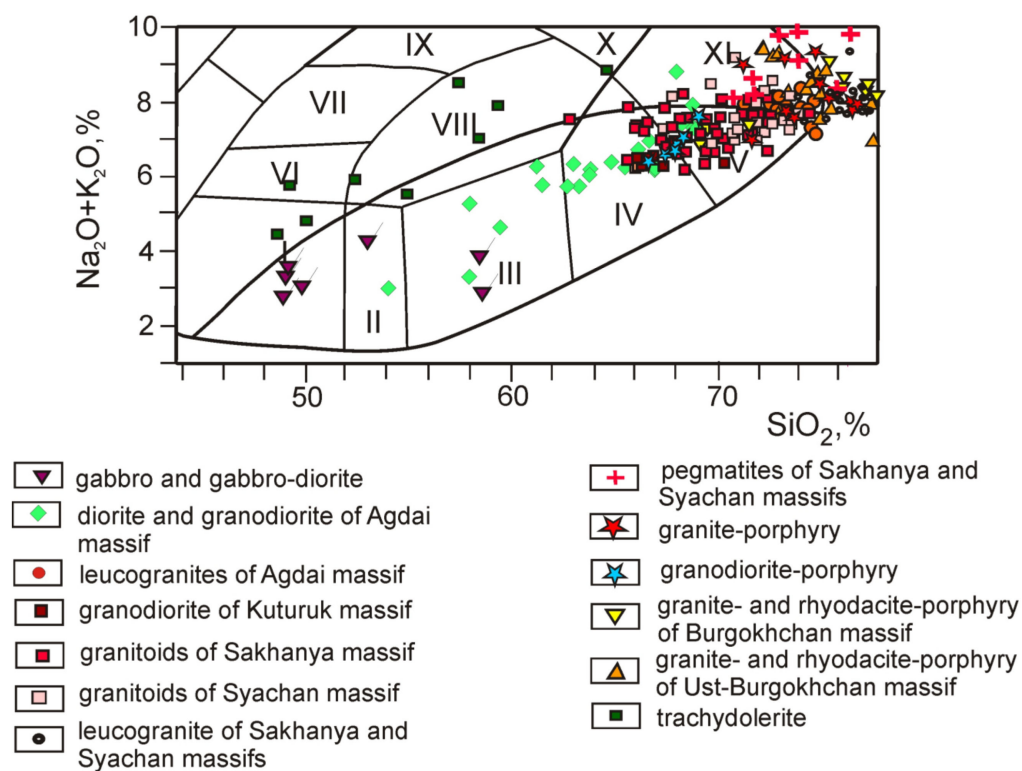


Figure 5. $\text{SiO}_2\text{--}(\text{Na}_2\text{O} + \text{K}_2\text{O})$ ratios in magmatic rocks of the Selennyakh River basin. Fields of the diagram [39]: I—gabbro; II—gabbro-diorites; III—diorites; IV—granodiorites; V—granites; VI—subalkaline gabbro; VII–VIII—monzonites; IX–X—syenites; XI—alkaline granites.

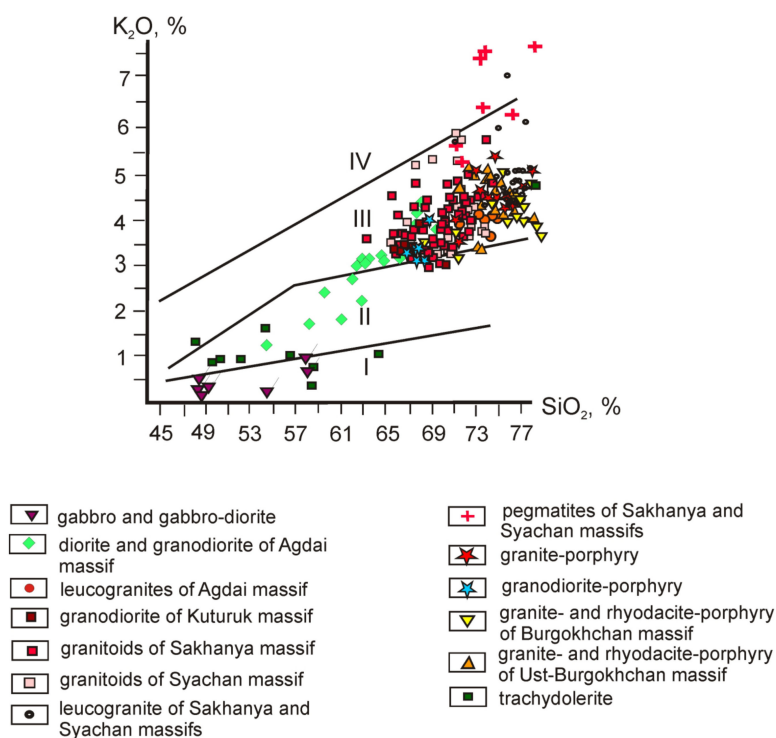


Figure 6. Petrochemical series of magmatic rocks of the Selennyakh River basin. Fields of the diagram [40]: I—low potassic tholeiitic, II—medium potassic calc-alkaline, III—high-potassic calc-alkaline, IV—shoshonite.

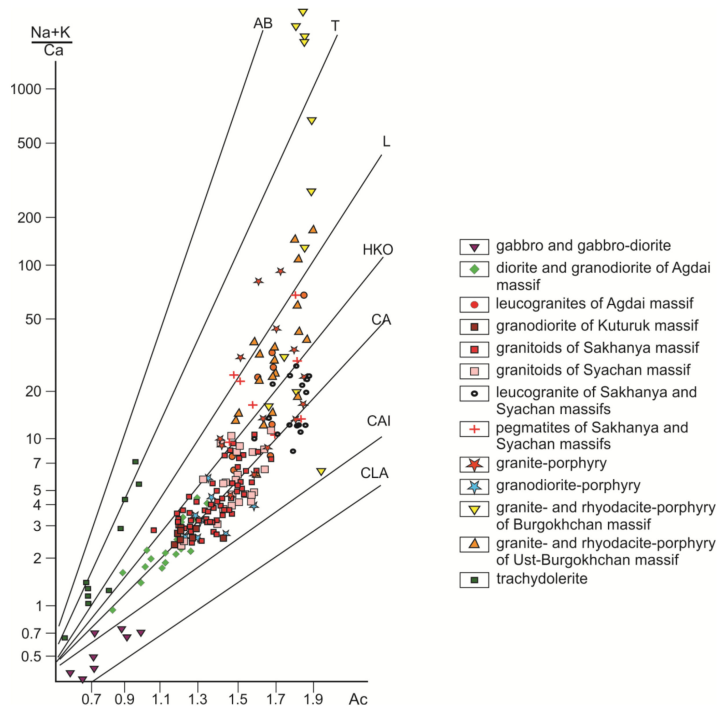


Figure 7. Magmatic series of magmatic rocks of the Selennyakh River basin. Symbols [41]: Ac—cation activity; trends of evolution: CAI—calcareous low-alkaline (island-arc), CA—calcareous-alkaline (crustal), HKO—high-potassium (orogenic), L—latite, T—trachite; AB—alkaline-basalt.

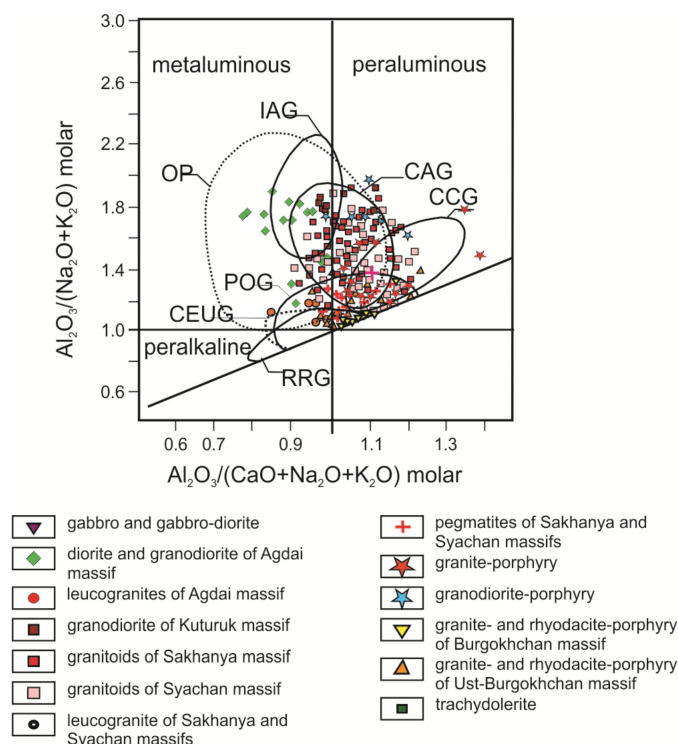


Figure 8. Alumina content in magmatic rocks of the Selennyakh River basin. Fields of the diagram [42]: OP—oceanic plagiogranites, IAG—*island-arc granitoids*, CAG—*granitoids of continental arcs*, CCG—*continental collision granitoids*, POG—*postorogenic granitoids*, CEUG—*granitoids of continental epirogenic uplift*, RRG—*riftogenic granitoids*.

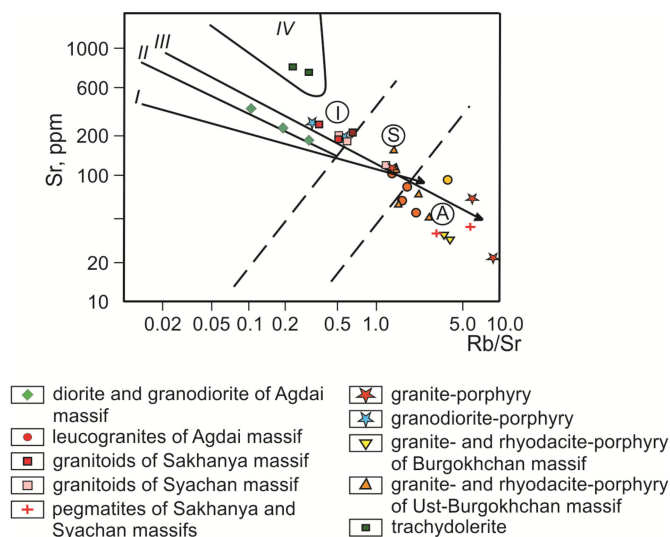


Figure 9. Sr-Rb/Sr ratios in magmatic rocks of the Selennyakh River basin. Trends of differentiation of typical series [43]: I—*tholeiitic island arcs*, II—*calcareous-alkaline island arcs*, III—*calcareous-alkaline active margins*, IV—*rift zones of continents*; I, S, A—*petrotypes of granitoids*.

The composition of the following age group of rocks (the beginning of the Early Cretaceous) was studied on the example of the eastern part of the Agdai massif. It varies from gabbro-diorites to granodiorites. Rocks are metaaluminous (Figure 8), of a low-potassium calc-alkali series (Figure 6). Their ferruginosity increases with the growth of SiO₂ from 54% to 83%. The normative composition is quartz-hypersthene-diopside, with a noticeable predominance of normative albite over orthoclase. Standard corundum is not

identified. $DI = 39\text{--}67\%$. According to the composition parameters, the rocks occupy an intermediate position between island-arc magmatic formations and magmatic formations of continental arcs and correspond to M-type suprasubduction granites [6].

The following temperatures of the parent melt calculated by different authors are close: $1000\text{--}1150\text{ }^{\circ}\text{C}$ [47], $1110\text{--}1155\text{ }^{\circ}\text{C}$ [37], $1007\text{--}1093\text{ }^{\circ}\text{C}$ [36]. The calculated magma generation pressure for the least differentiated samples is $10\text{--}12\text{ kbar}$ [38,47]. The temperature range of crystallization, determined by the ratios $\text{Al}_2\text{O}_3/\text{TiO}_2\text{--MgO}$ [47]— $1100\text{--}800\text{ }^{\circ}\text{C}$. The ratio of $\text{Al}/(\text{Mg} + \text{Fe})\text{--Ca}/(\text{Mg} + \text{Fe})$ in rocks (Figure 10) indicates the generation of the melt during the selective melting of amphibolites (Figure 10) [45].

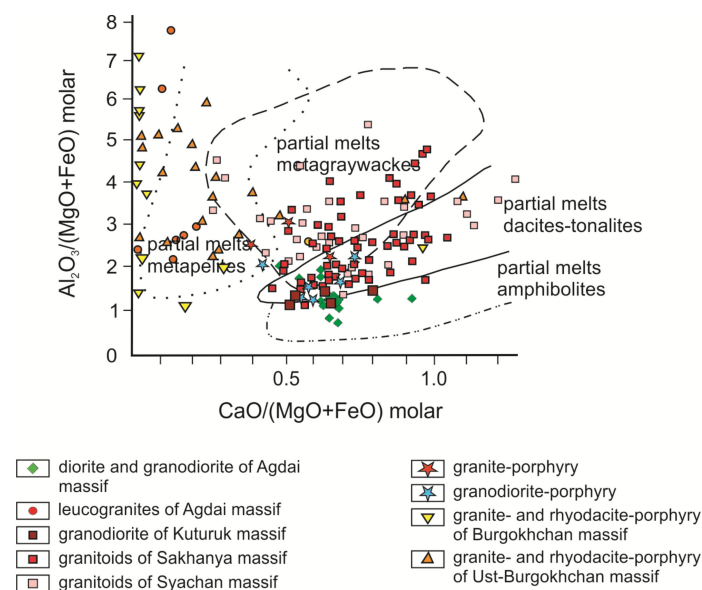


Figure 10. Magmogenesis substrates for igneous rocks of the Selennyakh River basin [45].

Granodiorites and granites of dikes are meta-aluminous (Schend index, $0.92\text{--}0.98$), ferruginous ($f = 66\text{--}84\%$), diopside-hypersthene normative, not containing normative corundum, with a predominance of normative albite ($31\text{--}58\%$) over orthoclase ($22\text{--}27\%$). $DI = 77\text{--}83\%$. The calculated magmogenesis temperatures are $907\text{--}931\text{ }^{\circ}\text{C}$ [36] at a pressure of $7\text{--}10\text{ kbar}$, and the variations in crystallization temperatures— $900\text{--}700\text{ }^{\circ}\text{C}$.

The igneous rocks of both associations considered above are metamorphosed near the contacts of large granitoid massifs. The chemical composition of the latter corresponds mainly to granodiorites and granites (Table S4, Figure 5). Rocks are diopside-hypersthene normative, with a slight predominance of normative albite over orthoclase (on average, $21\text{--}32\%$ and $16\text{--}27\%$, respectively).

Alkaline granites and quartz monzonites are developed in contact with carbonate rocks. All rocks are meta-aluminous or slightly supersaturated with alumina (Figure 8) and ferruginous ($f = 56\text{--}85\%$ in granitoids of the main facies and up to 100% —in leucocratic rocks of endocontacts). They belong to the high-potassium calc-alkali series (Figure 6) and, according to the composition parameters, correspond to granitoids of the I- or IS-type of continental arcs or granitoids of the calc-alkali series of active continental margins (Figures 8 and 9).

The calculated depth of magma generation [38] corresponds to a pressure of $9\text{--}11\text{ kbar}$. The $\text{Al}/(\text{Mg} + \text{Fe})\text{--Ca}/(\text{Mg} + \text{Fe})$ ratios in the rocks (Figure 10) correspond to the initiation of magma chambers at the boundary between dacite-tonalite and amphibolite substrates. The composition points of the least differentiated granitoids are localized within the melting field of amphibolite. Taking this into account, the maximum temperature of melts for the Kuturuk and Sakhanya massifs was determined at $1000\text{--}1020\text{ }^{\circ}\text{C}$, and for the Syachan massif at $960\text{--}980\text{ }^{\circ}\text{C}$ [36]. From the $\text{Al}_2\text{O}_3/\text{TiO}_2$ vs. MgO ratios [46], the crystallization

temperature of the first two massifs was estimated at 1000–650 °C and for the third massif at 900–630 °C, at a pressure of 9–2 kbar.

The aplites and leucogranites of dikes correspond in composition to alkali granites of the high-K calc-alkaline series (see Figures 5 and 6). They have a high ferruginosity (85–100%) and are metaluminous or weakly peraluminous (Figure 10). Pegmatites are distinguished by higher K contents with a transition from the high-K to shoshonitic series. The crystallization temperature of rocks of this group is 820–472 °C at 5–2 kbar. According to the Sr-Rb/Sr ratios, they are classified as A-type granites (Figure 9). The granite and granodiorite porphyries of the dikes differ from the rocks of the main facies of the massifs with corresponding SiO₂ contents only in the higher values of volatiles (H₂O, F, S, P). The maximum crystallization temperatures are 960 °C and 990 °C, and the maximum pressures during magma generation are 7.5 kbar and 9.4 kbar.

Magmatic formations of the following age group (the boundary of the Early and Late Cretaceous) are represented by the Burgokhchan, Ust-Burgokhchan massifs and the western part of the Agdai massif. Their chemical compositions correspond to granites and alkaline granites of the high-potassium calc-alkali series, with a transition to the shoshonite series of alkalinity (Figures 5 and 6). In the diagram of L. S. Borodin (Figure 7), the points of their compositions outline a trend that cuts through the main evolutionary trends. Granites are highly differentiated (DI = 84–97%), highly ferruginous (f = 87–100%), hypersthene normative, with a slight predominance of normative albite in the average compositions (34.9%, 30.5% and 30.2%, for granites of the Burgokhchan, Ust-Burgokhchan and Agdai massifs, respectively) over the orthoclase (23.4%, 25.8% and 23.1%, respectively), with low values of a normative corundum (0–0.6%). The normative composition of plagioclase is 1–14% an. Granites of all the massifs of this group are characterized by a moderate or slightly increased luminosity (Schend index from 0.85 to 1.2) (Figure 8). According to all the parameters of the composition, they are defined as postorogenic (intraplate) or rift-related granites of the A-type. The maximum calculated parameters of magmogenesis are close for the least differentiated differences of granites of all the massifs: 1032–996 °C [36] at a pressure of 6–9 kbar [38]. The temperature intervals of crystallization determined by the GCDkit program [7] for a series of samples using different geothermometers (Zr, apatite and REE saturation) were, for granites of the main facies of the Burgokhchan, Ust-Burgokhchan and Agdai massifs, respectively, 880–830 °C, 820–748 °C and 736–706 °C, and for endocontact—986–927 °C, 876–836 °C and 836–807 °C.

The composition of the latest igneous rocks of the territory is characterized by increased alkalinity and varies from sub-alkaline gabbro to monzonites and syenites. The rocks are mainly olivine-diopside normative, sometimes with a small amount of normative nepheline (12%), and a moderately aluminous, ferruginous (f = 50–85%), potassium-sodium type of alkalinity. The main parameters of the composition correspond to those of the rift-related derivatives of the trachyte series (Figures 7 and 9). The calculated parameters of magmogenesis are determined by different programs [37,46–48], close: P = 16–17 kbar, T = 1175–1220 °C.

6. Discussion

In the Late Jurassic period or at the turn of the Late Jurassic and Early Cretaceous period, the formation of small stocks and dikes of gabbro and dolerites occurred. The mineral and chemical features of the rocks (magnesian olivine with f = 16–18%, olivine-normative composition, low differentiation index DI = 24–27%, high magnesia) correspond to the generation of the parent melt under mantle conditions. According to the classification [44], they belong to the family of tholeiites and olivine tholeiites. According to the La/Yb–Yb ratios (5.4–2.4; 7.4–2.3), these rocks correspond to the derivatives of the mantle melt formed during the melting of slightly metasomatized spinel lherzolite [49]. The ratios in the rocks Ce/Sm–Ce (2.2–4.6; 2.8–4.7) indicate a low degree of its melting—2.5–3.5% [50]. According to the composition parameters, the geodynamic conditions of the formation of gabbroids are defined as close to the island-arc (suprasubduction) (Figures 6 and 7). The rocks contain

large grains of tschermakite hornblende framed by clinopyroxene. In experiments, such an amphibole was obtained at a pressure of more than 10 kbar and a temperature of about 800 °C. [51]. It is most typical for eclogites and garnet amphibolites and is practically not found in igneous rocks [52]. This allows us to assume the contamination of mantle melts by the substance of lower-crust substrates during magmogenesis. The values of primary Sr ratios ($I_0 = 0.7067\text{--}0.7069$), according to A.I. Zaitsev (17), also suggest the contamination of primary mantle melts by crustal matter.

The next stage of magmatic activity at the beginning of the Early Cretaceous was marked by the formation of massifs of complex composition, ranging from gabbro-diorites to granodiorites and similar M-type granitoids. The ratios in rocks $Al/(Mg + Fe)\text{--}Ca/(Mg + Fe)$ (Figure 10) and normalized values La/Yb (7.4, 5.7, 3.8)– Yb (8.5, 10, 10) [53], correspond to the origin of the parent melt in the amphibolite substrates of the lower crust. This is also confirmed by the presence of ferruginous tschermakite in diorites—a characteristic mineral of amphibolites. The variations in the $K/Rb\text{--}Rb$ (180–320) values also correspond to the generation of melts in substrates that were mantle matter or a mixture of crustal and mantle matter [54]. Thus, the actual material obtained indicates the origin of the parent melt for the East Agdai due to the selective melting of the lower crust amphibolites when they are exposed to the mantle basic melt and the latter is partially mixed with the resulting crustal melt.

In the next stage, the Early Cretaceous, the formation of granodiorite-granite massifs took place. The data of isotope analyses and geochemical features of the granitoids make it possible to attribute them to long evolved granitoids of continental arcs, formed in the conditions of an active continental margin (Figures 8 and 9). Magma chambers were formed within the lower crustal amphibolites or at the boundary between the amphibolite and dacite-tonalite substrates (Figure 10) at a pressure of 9–11 kbar and a temperature of 1020–990 °C. Low chondrite-normalized La/Yb values (2.9–5.6) also testify to magma generation in amphibolite substrates [53]. The presence of basic rocks in magma-forming substrates is also indicated by the high content of pyrope mineral in accessory garnet, restite zircons of morphotype D, and K/Rb values (200–400) in granitoids. According to experimental data [55,56], melting amphibolites can lead to the formation of granitoid melts in the presence of a fluid phase (primarily H_2O and $NaCl$), which agrees well with the high water content (913–1025 mg/kg) in magmatogenic inclusions and the composition of water extracts from the quartz of granitoids of the studied massifs ($Na^+ = 12\text{--}16$ mg-eq/l, $Cl^- = 13\text{--}27$ mg-eq/l [57]). According to the composition parameters, granitoids belong to the I- or IS-type.

Granodiorite- and granite-porphyrries differ from the rocks of the main facies of the massifs with a corresponding SiO_2 content only in higher contents of volatiles (H_2O , F, S, P) (Table S4). The maximum temperatures and pressures of their magma generation (990 °C and 960 °C at 9.4 kbar and 7.5 kbar) are also comparable. The retention of high temperatures of melt formation to the latest derivatives requires the supply of juvenile heat and fluids to the root parts of magma chambers during the process of the formation of granitoid massifs.

At the turn of the Early and Late Cretaceous, the formation of the western part of the Agdai massif and the Burgokhchan and Ust-Burgokhchan massifs began. The alkali-feldspar granites and leucogranites composing them are defined by all the geochemical parameters as postorogenic or rift-related A-type granites. Calculated pressures during magmogenesis (6–9 kbar), features of Rb-Sr isotope systems $I_0 = 0.71053\text{--}0.72540$ indicate the crust nature of the protoliths. At the same time, high melt temperatures (up to 1032 °C) at such low pressures could be achieved only when additional heat was supplied to the magmogenesis levels from an external source. Granites are characterized by a combination of high-temperature minerals characteristic of the basic rocks (clinopyroxene with parameters of clinopyroxenes of basite-hyperbasite and picrite-basalt associations, titanomagnetite, magnesian ilmenite, zircon of D morphotype) and low-temperature, typi-

cally granite, minerals (oligoclase-albite, manganous ilmenite, F-apatite, fluorite). Taken together, these data indicate a mixed (syntexis) origin of the parent melts.

In Figure 11, the points of the granite compositions of the massifs of this group are localized in the field of A1 granites, the formation of which is related to plumes or hot spots and continental rifts [58]. This is consistent with the opinion of the majority of researchers who have dealt with the problems of A-granites, who have shown that such high temperatures are usually not reached in the earth's crust; that is, "the involvement of mafic magmas, or high mantle heat flows, is a necessity" for the generation of melts forming A-type granites [59,60].

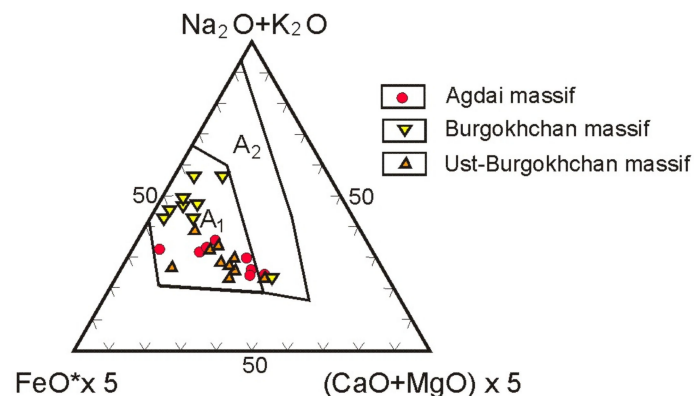


Figure 11. Ratios of molar values of petrochemical components in granites of the Selennyakh River basin. Diagram fields [58]: A₁—granites of oceanic islands, continental rifts and hotspots formed from a basaltic source of oceanic islands, intraplate, or rift environments; A₂—post-collisional, post-orogenic and anorogenic granites formed from a basaltic source of island arcs and continental margins, or a crustal source of tonalite and granodiorites, or by partial melting of the crust.

The latest intrusive formations of the territory are represented by a sub-alkaline gabbro, trachydolerites and trachyandesites of the trachyte series of rift-related continental geodynamic conditions. Compared with rocks of the Late Jurassic with similar SiO₂ contents, they are characterized by an increased alkalinity, and higher deeper magmogenesis conditions (pressure up to 17.9 kbar). According to the La/Yb–Yb ratios (17–1.6 and 23–2.1), the rocks correspond to the derivatives of melts formed during the melting of metasomatically enriched lherzolite [49].

Thus, in the course of the evolution of the Late Mesozoic magmatism of the Selennyakh block of the Omulevka terrane, there was a change of the Late Jurassic magmatism, close to the island-arc (suprasubduction) magmatism, by the Early Cretaceous magmatism of the continental arcs of active margins and at the turn of the Early and Late Cretaceous by continental rift-related magmatism. At the same time, there was a change basically of the main magmatism to more and more silicic acid and more alkaline (an increase in the total alkalinity—Figure 5) with the movement of magmogenesis levels to higher and higher horizons of the lithosphere, but with the preservation of close high magmogenesis temperatures. The magmatic activity within the territory ends in the very end of the Late Cretaceous with the formation of dikes—derivatives of melts of the metasomatized mantle. At the same time, all the studied igneous rocks are either direct mantle derivatives, or bear signs of the participation of mantle matter in the generation of melts in crustal substrates. On the A–B diagram of F. Debon and P. LeFort (Figure 12), the overwhelming number of points of their compositions is localized along the mixing trend [61]. The article presents the results of the study of Late Mesozoic intrusive formations of the Omulevka terrane of the Verkhoyansk–Kolyma orogenic region. The research area covers the Selennyakh block of the Omulevka terrane and the territory adjacent to the south. The compositions of rock-forming, accessory and restitic minerals and geochemical features of intrusive rocks are considered. The methods of optical microscopy, microprobe, silicate and spectral

analyses were used. There are several stages in the evolution of magmatism as follows: (1) the Late Jurassic supra-subduction (gabbro, dolerites), (2) the beginning of the Early Cretaceous-transitional from supra-subduction to marginal-continental (gabbro-diorites, diorites, granodiorites), (3) the Early Cretaceous of active continental margin (granodiorites, granites), (4) the Late Cretaceous postorogenic or continental-riftogenic (alkali-feldspar granites of A-type), (5) the Late Cretaceous continental riftogenic (subalkaline gabbroids and basaltoids). In the process of evolution from stage one to stage four, there was an increase in the silicic acid content, total alkalinity and ferruginosity of the rocks with the movement of magmogenesis levels to higher and higher horizons of the lithosphere (calculated pressure from 1.6–1.4 GPa to 0.6–0.9 GPa). At the same time, the preservation of high temperatures of magmogenesis (1000–1150 °C) and crystallization implies the supply of additional heat from an external (deep) source during the formation of granitoid melts. The magmatic activity is completed by the intrusion of subalkaline derivatives of a deep hearth, formed by metasomatized lherzolites. All the studied igneous rocks are either direct mantle fusions, or bear signs of the participation of mantle matter in the generation of parent melts in crustal substrates: the presence of tschermakite in gabbroid, nonequilibrium structures, the composition of early generations of biotites corresponding to biotites of mantle and crust–mantle derivatives, the presence of pyroxenes and accessory minerals characteristic of mantle magmas—in granitoids. In the diagram of Al–Na–K–2Ca–Fe + Ti + Mg, the composition points of the studied intrusive rocks tend to the mixing trend. In general, the research results suggest that the evolution of the Late Mesozoic intrusive magmatism of the studied territory and the specific matter of rock compositions were caused by the crust–mantle interaction as a result of the rise of mantle diapirs into the crust from a long-existing deep hearth of the main melt.

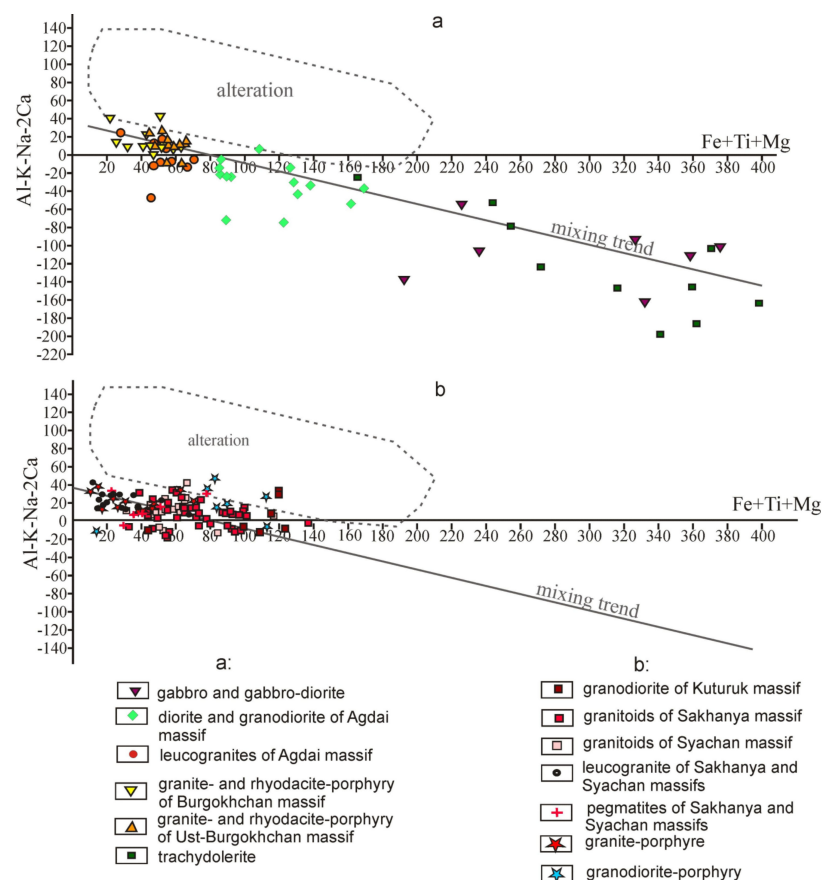


Figure 12. a–b diagram for the magmatic rocks of the Selennyakh River basin: (a) = $Al - (K + Na + 2Ca)$; (b) = $Fe + Ti + Mg$ —in gram-atoms [61].

The actual and analytical material obtained in the course of research allows us to assume the presence of buried foci of the main melts within the studied territory, the repeated activation of which caused the melting of crustal substrates in the late Mesozoic. These conclusions are consistent with the results of long-term geothermal and geophysical studies, on the basis of which G. A. Stogniy and V. V. Stogniy identified the Verkhoyansk–Kolyma regional anomaly of increased heat flow due to mantle diapirism or the presence of a plume [62]. E.A. Korago adheres to a similar point of view, linking the Late Paleozoic–Mesozoic history of Northeast Asia with the influence of the mantle diapir centered in the Kolyma loop [63].

7. Conclusions

The duration of the evolution of the Late Mesozoic intrusive magmatism of the Selennyakh block of the Omulevka terrane until the end of the Late Jurassic to the Late Cretaceous and Paleogene is defined. The following are the several stages in the evolution of magmatism: (1) the Late Jurassic (or the boundary of the Jurassic and Cretaceous) suprasubduction (gabbro, dolerites), (2) the beginning of the Early Cretaceous transition from suprasubduction to marginal-continental (gabbro-diorites, diorites, granodiorites), (3) the Early Cretaceous active continental margin (granodiorites, granites), (4) the Late Cretaceous postorogenic or continental-rift-related (alkaline-feldspar granites of A-type), (5) the Late Cretaceous continental rift-related stage (sub-alkaline gabbroids and basaltoids). In the process of evolution from stage one to stage four, there was an increase in the content of SiO₂, total alkalinity and ferruginosity of rocks with the movement of magmogenesis levels to higher and higher horizons of the lithosphere (calculated pressure from 1.2–1.4 GPa to 0.6–0.9 GPa). At the same time, the preservation of high magmogenesis temperatures (1000–1150 °C) requires additional heat from an external (deep) source. Magmatic activity within the territory is completed in the Late Cretaceous–Paleogene by the intrusion of subalkaline derivatives of a deep hearth formed by metasomatized lherzolites.

All the studied igneous rocks are either direct mantle derivatives, or bear signs of the participation of mantle matter in the generation of melts in crustal substrates: the presence of chermakite in gabbroids, nonequilibrium structures and the presence of pyroxenes and accessory minerals characteristic of mantle magmas in granitoids, the composition of early generations of granitoid biotites corresponding to biotites of mantle and crustal-mantle derivatives; localization of rock composition points along the mixing trend in the F. Debon and P. LeFort A–B diagram.

The results of this research suggest that the evolution of the Late Mesozoic intrusive magmatism of the studied territory and the specific nature of the rock compositions were due to the crust-mantle interaction as a result of the rise of mantle diapirs into the crust from a long-existing deep hearth.

Supplementary Materials: The following are available online at <https://www.mdpi.com/article/10.3390/min1111208/s1>, Table S1: Contents of major (wt.%) elements in pyroxenes of magmatic rocks of Selennyakh Ridge, Table S2: Contents of major (wt.%) elements in amphiboles of magmatic rocks of Selennyakh Ridge, Table S3: Contents of major (wt.%) elements in biotites of magmatic rocks of Selennyakh Ridge, Table S4: Contents of major (wt.%) elements in magmatic rocks of Selennyakh Ridge, Figure S1: Route diagram and numbers of observation points.

Funding: This research was funded by DPMGI SB RAS (project no. FUEM-2019-0001).

Acknowledgments: The author expresses gratitude to all who performed analytical research. Special thanks are due to Special thanks to A.V. Prokopiev for his help in preparing the article for publication, M.I. Ivanov and A.I. Zhuravlev for their help in preparing the graphic material and the technical edition of the article. Field, analytical works and interpretation are supported by project of the DPMGI SB RAS.

Conflicts of Interest: The author declares no conflict of interest.

References

1. Parfenov, L.M.; Kuzmin, M.I. (Eds.) *Tectonics, Geodynamics and Metallogeny of the Territory of the Republic of Sakha (Yakutia)*; MAIK “Nauka/Interperiodika”: Moscow, Russia, 2001. (In Russian)
2. Nekrasov, I.Y. *Magmatism and Ore Deposits of the Northwestern Verkhoyansk-Chukotka Fold. Area*; Nauka: Moscow, Russia, 1962. (In Russian)
3. Ivensen, Y.P.; Amuzinskiy, V.A.; Nevoisa, G.G. *Structure, Formation History, Magmatism, and Metallogeny of the Northern Verkhoyansk Folded Zone*; Nauka: Novosibirsk, Russia, 1975. (In Russian)
4. Grinberg, G.A.; Bakharev, A.G.; Gamyarin, G.N.; Nukhtinskiy, G.G.; Nedosekin, Y.D. *Granitoids of the South. Verkhoyansk Region*; Nauka: Moscow, Russia, 1970. (In Russian)
5. Shkodzinskiy, V.S.; Nedosekin, Y.D.; Surnin, A.A. *Petrology of Late Mesozoic Magmatic Rocks of Eastern Yakutia*; Nauka: Novosibirsk, Russia, 1992. (In Russian)
6. Trunilina, V.A.; Roev, S.P.; Orlov, Y.S. *Granitoids of the Batholithic Belts in the Northeastern Verkhoyansk-Kolyma Mesozoids*; 658 Media-Holding “Yakutia”: Yakutsk, Russia, 2013. (In Russian)
7. Janoušek, V.; Farrow, C.M.; Erban, V. Interpretation of whole-rock geochemical data in igneous geochemistry: Introducing Geochemical Data Toolkit (GCDkit). *Petrology* **2006**, *47*, 1255–1259. [[CrossRef](#)]
8. Carr, M.J. *Igpet for Windows*; Terra Softa Inc.: Somerset, NJ, USA, 2010.
9. Korinevsky, E.V. PetroExplorer—a new computer program for storing and calculating chemical analyses of minerals and rocks. In *Abstracts of the VI International School of Earth Sciences Named after L. L. Perchuk*; Institute of Mineralogy UB RAS: Odessa, Ukraine, 2010; pp. 63–66. (In Russian)
10. Saranchina, G.M.; Kozhevnikova, V.N. *Fedorovsky Method: Determination of Minerals, Microstructural Analysis*; Nedra: Leningrad, Russia, 1985. (In Russian)
11. Baraz, V.R.; Levchenko, V.P.; Povzner, A.A. *Structure and Physical Properties of Crystals*; Ural State University: Yekaterinburg, Russia, 2009. (In Russian)
12. Nokleberg, W.J. (Ed.) Metallogenesis and tectonics of northeast Asia. *U.S. Geological Survey Professional Paper* **1765**, 2010.
13. Toro, J.; Miller, E.L.; Prokopiev, A.V.; Xiaojing, Z.; Veselovskiy, R. Mesozoic orogens of the Arctic from Novaya Zemlya to Alaska. *J. Geol. Soc.* **2016**, *173*, 989–1006. [[CrossRef](#)]
14. Layer, P.V.; Newberry, R.; Fujita, K.; Parfenov, L.M.; Trunilina, V.A.; Bakharev, A.G. Tectonic setting of the plutonic belts of Yakutia, Northeast Russia, based on ⁴⁰Ar/³⁹Ar and trace element geochemistry. *Geology* **2001**, *29*, 167–170. [[CrossRef](#)]
15. Akinin, V.V.; Miller, E.L.; Toro, J.; Prokopiev, A.V.; Gottlieb, E.S.; Pearcey, S.; Polzunenkov, G.O.; Trunilina, V.A. Episodicity and the dance of late Mesozoic magmatism and deformation along the northern Circum-Pacific margin: NE Russia to the Cordillera. *Earth-Sci. Rev.* **2020**. [[CrossRef](#)]
16. Stavskiy, A.P.; Ged’ko, M.I.; Danilov, V.G. The Uyandina-Yasachnaya island arc. In *Geological Mapping of Volcano Plutonic Belts*; Nedra: Moscow, Russia, 1994; pp. 265–297. (In Russian)
17. Trunilina, V.A.; Roev, S.P.; Orlov, Y.S. *Volcanic-Plutonic Belts of the North-East of Yakutia*; Yakutsk: Sakhapoligrafizdat, Russia, 2007. (In Russian)
18. Nenashev, N.I.; Zaitsev, A.I. *Geochronology and Problem of Genesis of Granitoids of East. Yakutia*; Nauka: Novosobirsk, Russia, 1980. (In Russian)
19. Yavuz, F. Win Pyrox: A Windows program for pyroxene calculation classification and thermobarometry. *Am. Mineral.* **2013**, *98*, 1338–1359. [[CrossRef](#)]
20. Rudolphi, R.; Renzulli, A. Calcic amphiboles in calc-alkaline and alkaline magmas: Thermobarometric and chemometric empirical equations valid up to 1130 °C and 2. 2 Gpa. *Contrib. Mineral. Petrol.* **2012**, *163*, 877–895. [[CrossRef](#)]
21. Hammerstrom, J.M.; Zen, E. Aluminium in Hbl an empirical igneous. *Am. Mineral.* **1986**, *71*, 1297–1313.
22. Uchida, E.; Endo, S.; Makino, V. Relationship between solidification depth of granitic rocks and formation of hydrothermal ore deposits. *Resour. Geol.* **2007**, *57*, 47–56. [[CrossRef](#)]
23. Henry, D.A.; Guidotti, C.V.; Thompson, J.A. The Ti-saturation surface for low-to-medium pressure metapelitic biotites: Implication for geothermometry and Ti-substitution mechanism. *Am. Mineral.* **2005**, *90*, 316–328. [[CrossRef](#)]
24. Troshin, Y.P.; Grebenshchikova, V.I.; Antonov, A.Y. Volatile components in biotites and metallogenic specialization of intrusions. In *Mineralogical Criteria for Ore Content Assessment*; Nauka: Leningrad, Russia, 1981; pp. 73–83. (In Russian)
25. Wones, D.R.; Eugster, H.P. Stability of biotite: Experiment, theory and application. *Am. Mineral.* **1985**, *9*, 1228–1272.
26. Tindle, A.G.; Webb, R.P. Estimation of lithium contents in trioctahedral micas using microprobe data: Application to micas from granitic rocks. *Eur. J. Mineral.* **1990**, *2*, 595–610. [[CrossRef](#)]
27. Brown, G.G. A comment on the role of water in the partial fusions of crystal rocks. *Earth Planet. Sci. Lett.* **1970**, *9*, 355–358. [[CrossRef](#)]
28. Brimhall, G.H.; Crerar, D.A. Ore fluids: Magmatic to supergene. In *Thermodynamic modeling of geological materials. Minerals, Fluids and Melts. Rev. Mineral. Geochem. Mich.* **1987**, *17*, 235–321.
29. Bushlyakov, I.N.; Kholodnov, V.V. *Halogens in Petrogenesis of Granitoids*; Nedra: Moscow, Russia, 1986. (In Russian)
30. Gusev, A.I. Tipizatziia granitoidov na osnove sostavov biotitov. *Uspekhi Sovrem. Estestvozn.* **2010**, *4*, 54–57. (In Russian)
31. Brown, G.G.; Parsons, J. Calorimetric and phase-diagram approaches to two-feldspar geothermometry: A critique. *Am. Mineral.* **1985**, *70*, 336–351.

32. Pupin, J.P. Zircon and Granite Petrology. *Contrib. Mineral. Petrol.* **1980**, *73*, 207–220. [[CrossRef](#)]
33. Popov, V.S. Garnet composition as an indicator of the genesis of calcareous-alkaline igneous rocks. *Izv. USSR Academy Sci.* **1982**, *3*, 36–46. (In Russian)
34. Putirka, K.D. Igneous thermometers and barometers based on plagioclase + liquid equilibria: Tesis of some existing models and new calibrations. *Am. Mineral.* **2005**, *90*, 336–346. [[CrossRef](#)]
35. Ryabov, V.V.; Zolotukhin, V.V. *Minerals of Differentiated Traps*; Nauka: Novosibirsk, Russia, 1977. (In Russian)
36. Jung, S.; Pfander, J.A. Source composition and melting temperatures of orogenic granitoids—constraints from CaO/Na₂O, Al₂O₃/TiO₂ and accessory mineral saturation thermometry. *Eur. J. Mineral.* **2007**, *1*, 5–40.
37. French, W.J.; Cameron, E.P. Calculation on the temperature of crystallization of silicates from basaltic melts. *Mineral. Mag.* **1981**, *44*, 19–26. [[CrossRef](#)]
38. Belyaev, G.M.; Rudnik, V.A. *Formational-Genetic Types of Granitoids*; Leningrad: Nedra, Russia, 1978. (In Russian)
39. Wilson, M. *Igneous Petrogenesis*; Unwin Hayman: London, UK, 1989.
40. Whiteford, D.G.; Nicholls, I.A.; Taylor, S.R. Spatial variations in the geochemistry of Quaternary lavas across the Sunda arc in Java and Bali. *Contrib. Mineral. Petrol.* **1979**, *70*, 341–356. [[CrossRef](#)]
41. Borodin, L.S. *Petrochemistry of Magmatic Series*; Nauka: Moscow, Russia, 1987. (In Russian)
42. Maniar, P.D.; Piccoli, P.M. Tectonic discrimination of granitoids. *Geol. Soc. Am. Bull.* **1989**, *101*, 635–643. [[CrossRef](#)]
43. Datsenko, V.M. Petrogeochemical typification of granitoids of the south-western framing of the Siberian platform. In *Materials of the Second All-Russian Petrographic Meeting*; Komi SC UB RAS: Syktyvkar, Russia, 2000; Volume 2, pp. 270–274. (In Russian)
44. Williams, H.; Turner, F.; Gilbert, C. *Petrography*; Moscow: Mir, Russia, 1985. (In Russian)
45. Gerdes, A.; Worner, G.; Henk, A. Post-collisional granite generation and HT-LP metamorphism by radiogenic heating: The Variscan South Bohemian Batholith. *Geol. Soc. Lond.* **2000**, *157*, 577–587. [[CrossRef](#)]
46. Perchuk, L.L.; Aranovich, L.A.; Kosyakova, N.A. Thermodynamic models of the origin and evolution of basalt magmas. *Vestnik MSU. Geology* **1982**, *4*, 3–26. (In Russian)
47. Kulikova, V.V.; Kulikov, V.S. *Petrochemical Classification of Magmatic Rocks*; Kola Scientific Center: Petrozavodsk, Russia, 2001. (In Russian)
48. Piskunov, B.M.; Abdurakhmanova, A.I.; Kim, C.U. Composition-depth ratio for volcanoes of the Kuril island arc and its petrological significance. *Volcanol. Seismol.* **1979**, *4*, 57–67. (In Russian)
49. Drill, S.I.; Kuzmin, M.I.; Tsipukova, S.S.; Zonenshain, L.P. Geochemistry of basalts from the West Woodlark, Lau and Manus basins: Implication for their petrogenesis and source rock composition. *Mar. Geol.* **1997**, *142*, 57–83. [[CrossRef](#)]
50. Rollinson, H.R. *Using Geochemical Data: Evaluation, Presentation, Interpretation*; Longman Group Limited: London, UK, 1995.
51. Plyusnina, L.L. Experimental calibration of a clinopyroxene-amphibole geothermometer. *Rep. USSR Acad. Sci.* **1985**, *280*, 723–727. (In Russian)
52. Kostyuk, E.A. Amphiboles. In *Genetic Studies in Mineralogy*; SB of the USSR Academy of Sciences: Novosibirsk, Russia, 1980; pp. 144–155. (In Russian)
53. Djan, B.-M.; Chjan, Z.K. Radiometric age (Rb-Sr, Sm-Nd, U-Pb) and geochemistry of rare earth elements in Archean granulitic gneiss of Eastern Hebei province, China. In *Geochemistry of Archean*; Nauka: Moscow, Russia, 1987; pp. 250–284. (In Russian)
54. Rub, M.G.; Ashikhmina, N.A.; Gladkov, N.I. Typomorphic features of accessory minerals and their significance for identification of genesis and ore content of granitoids. In *Granitoids of Folded and Activated Regions and Their Ore Content*; Nauka: Moscow, Russia, 1977; pp. 197–235. (In Russian)
55. Beard, J.S.; Lofgren, G.E. Effect of water on the composition of partial melts of greenstone and amphibolite. *Science* **1989**, *244*, 195–197. [[CrossRef](#)] [[PubMed](#)]
56. Khodorevskaya, L.I. Granitization of amphibolites. 2. Basic laws of physical and chemical phenomena in the processes of fluid filtration through the rock. *Petrology* **2004**, *12*, 321–336. (In Russian)
57. Trunilina, V.A. *Geology and Ore Content of Late Mesozoic Magmatic Formations in Northeast Yakutia*; Novosibirsk: Nauka, Russian, 1992. (In Russian)
58. Grebennikov, A.V. Granitoids of A-type: Problems of diagnostics, formation and systematics. *Geol. Geophys.* **2014**, *55*, 1356–1373. (In Russian)
59. Eby, G.N. Chemical subdivision of the A-type granitoids: Petrogenetic and tectonic implications. *Geology* **1992**, *20*, 641–644. [[CrossRef](#)]
60. King, P.L.; White, A.J.R.; Chappell, B.W.; Allen, C.M. Characterization and Origin of aluminous A-type Granites from the Lachan Fold Belt, Southeastern Australia. *Petrology* **1997**, *38*, 371–391. [[CrossRef](#)]
61. Debon, F.; Le Fort, P. A cationic classification of common plutonic rocks and their magmatic associations: Principles, method, applications. *Bull. Minéral.* **1988**, *111*, 493–510. [[CrossRef](#)]
62. Stogniy, G.A.; Stogniy, V.V. *Geophysical Fields of the Eastern Part of the North. Asian Craton*; Yakutsk: Sakhapoligrafizdat, Russia, 2005. (In Russian)
63. Korago, E.A. Model of tectonics of Northeast Asia from the position of mantle diapirism. In *Thrusts and Surges of Platform and Folded Regions of Siberia and The Far East. and Their Metallogenic Significance*; SB RAN: Irkutsk, Russia, 1992; pp. 112–114. (In Russian)